

## A COMPARATIVE STUDY ON THE INITIAL IN-PLANE STIFFNESS OF MASONRY WALLS WITH OPENINGS

A. Shabani<sup>(1)</sup>, V. Plevris<sup>(2)</sup>, M. Kioumarsi<sup>(3)</sup>

<sup>(1)</sup> PhD Candidate, Department of Civil Engineering and Energy Technology, Oslo Metropolitan University, Oslo, Norway, [amirhose@oslomet.no](mailto:amirhose@oslomet.no)

<sup>(2)</sup> Associate Professor, Department of Civil and Architectural Engineering, Qatar University, Doha, Qatar, [vplevris@qu.edu.qa](mailto:vplevris@qu.edu.qa)  
Professor, Dept. of Civil Engineering and Energy Technology, Oslo Metropolitan University, Oslo, Norway, [vageli@oslomet.no](mailto:vageli@oslomet.no)

<sup>(3)</sup> Associate Professor, Department of Civil Engineering and Energy Technology, Oslo Metropolitan University, Oslo, Norway, [mahdik@oslomet.no](mailto:mahdik@oslomet.no)

### Abstract

Masonry buildings have been used for centuries in various locations around the world, including areas with high seismicity. Studies about the behavior of masonry structural components subjected to lateral loadings and retrofitting techniques for improving their performance have gained much attraction lately. Various simplified methods have been presented in the literature for the seismic vulnerability assessment of masonry buildings. The initial in-plane stiffness of masonry walls is a key parameter which significantly affects the nonlinear backbone curve of the masonry walls as well as their ultimate in-plane strength.

Different simplified analytical methods have been proposed for deriving the initial in-plane stiffness of masonry buildings with regular or irregular openings by considering the flexible spandrels that can translate and rotate under lateral load and flexible piers' endings. In the analytical methods, the initial in-plane stiffness of each pier will be computed from the equations by considering the geometry of each component as input. Each structural component is considered as a spring and the stiffness of the whole system is computed based on equations of springs in series or in parallel.

The finite element method is considered as a reliable tool for verifying the analytical methods. For this purpose, a homogenization method has been employed for modeling the masonry walls and lateral loads have been applied on the walls with the assumption of linear material to derive the initial in-plane stiffness of the walls. For this purpose, three categories of masonry walls have been considered with one, two, and three openings where the openings' geometries also vary to investigate the effect of opening placements and irregularities on the initial in-plane stiffness of the walls. Afterwards, the stiffnesses computed from the analytical methods are compared with the stiffnesses that have been derived from the finite element analysis to investigate the accuracy of the analytical methods. It is shown that the analytical methods can be utilized for deriving the initial in-plane stiffness of masonry walls with openings, providing fast and accurate solutions in comparison to more detailed and time-consuming finite element implementations.

*Keywords: Initial stiffness; masonry walls; in-plane stiffness; analytical methods; finite element analysis*

## 1. Introduction

Unreinforced masonry (URM) buildings can be considered as the oldest construction technique in the world [1] that consists of URM shear walls as a load-bearing system [2, 3]. Moreover, nowadays, URM walls have been utilized in moment-resisting frames as an infill wall, effective on the building responses to the different types of loadings [4, 5]. The initial in-plane stiffness (IIPS) of each structural component is considered as a key parameter for design purposes and deriving the nonlinear analysis's backbone curve [6, 7], which is significantly effective on the nonlinear analysis results. Therefore, calculating an accurate enough value for the IIPS of URM walls could be critical for seismic performance evaluation of URM buildings [8-10] and designing the modern buildings with URM infill walls [11]. Instead of performing finite element (FE) analysis, different analytical hand methods have been developed for the estimation of IIPS of URM walls with less computational effort. For the URM walls without openings, the estimation of the IIPS by assuming the wall as a deep beam is easy and accurate enough since rigid boundary conditions are considered in both the theory and equations. Nevertheless, in terms of perforated URM walls, the estimation of this parameter is not accurate enough due to the possible flexibility of pier ends [9].

As the easiest method for the estimation of the IIPS of URM walls with openings, the wall is discretized to piers, and the IIPS of each pier can be derived based on the deep beam theory neglecting the flexible boundary conditions. It was investigated that the perforated wall's IIPS is overestimated using this method [9]. Another well-known analytical hand method is called the interior strip method [12]. By comparing the results with the results of FE analysis, it was investigated that the interior strip method is not accurate enough and overestimate the IIPS of the perforated URM wall in some cases [12]. Moreover, an analytical method was proposed in [13] considering flexible endings for piers by modifying the boundary conditions stiffnesses, and design tables were provided to facilitate the estimation process of the IIPS. The method's accuracy was then verified by comparing the results with the FE analysis results [13, 14]. Furthermore, the effective height method is an analytical method proposed in [9]. Modification of the pier stiffness due to the flexible boundary conditions has been performed using regression analysis based on the FE analysis of cantilever piers with different boundary conditions. The method has been validated by comparing the results with the FE analysis results of four perforated walls [9].

The last two mentioned analytical methods are chosen in the current study to investigate their performance against the FE analyses. Due to the low number of case studies investigating the performance of the methods in previous studies, a broader level of URM walls with different configurations of openings is needed to be developed. Firstly, a FE model has been developed and validated based on an experimental test performed by [15]. Afterward, URM wall case studies with openings in different configurations have been modeled and analyzed. Then, the IIPS of the walls is derived based on the modified boundary conditions stiffness method and the effective height method. Finally, the results from the two analytical methods have been compared with the FE analysis results to determine each analytical method's accuracy, and modifications have been proposed to improve the accuracy of the analytical methods.

## 2. Method

In this section, details about all the analysis types for estimating IIPS of URM walls are presented and investigated. Firstly, the experimental test is presented as the most robust method. Then the FE modeling procedure and the procedure of the two analytical methods utilized in this study are presented.

### 2.1 Experimental test

Quasi-static and monotonic tests on a single-leaf tuff masonry URM wall with an opening were performed by [15], where the geometrical data of the tested wall is shown in Figure 1. Vertical forces of 200 kN were applied to the piers by hydraulic jacks to simulate gravity loads [16]. A prescribed monotonic displacement was applied on one side of the wall through the test procedure, and the horizontal resistant force of the wall and the deformation were recorded.

## 2.2 FE modeling

Different methods have been presented for the numerical modeling of URM walls. Among them, the continuum-based method is utilized in this study. In this method, the masonry unit will be considered as a homogenous texture, and the masonry blocks and mortar joint have not been modeled in detail [2].

Based on a database from the test to derive the shear modulus ( $G$ ) of masonry, see [17], it is concluded that  $G=0.15E$ , where  $E$  is the modulus of elasticity. This is a reasonable estimation equation for calculating the accurate enough  $G$  parameter. Using  $G=0.4E$  by assuming the masonry as an isotropic material overestimates the  $G$  parameter and the URM wall's stiffness [17]. The FE model of the test wall has been developed in DIANA FEA software [18] considering the mentioned assumptions with the material properties summarized in Table 1.

Table 1 – Material properties of masonry for the FE model validation.

	E(GPa)	G(GPa)	$\rho$ (kg/m <sup>3</sup> )
Tuff masonry (compression parallel to bed joints)	2.07	0.31	1600
Tuff masonry (compression perpendicular to bed joints)	2.22		

Furthermore, two blocks on top of each pier have been modeled to simulate the test set up with a specific density to simulate the constant vertical applied load of 200 kN as illustrated in Fig.1 [16]. However, it was investigated that the effect of vertical loads in FE analysis is negligible on the IIPS of URM walls, see [13].

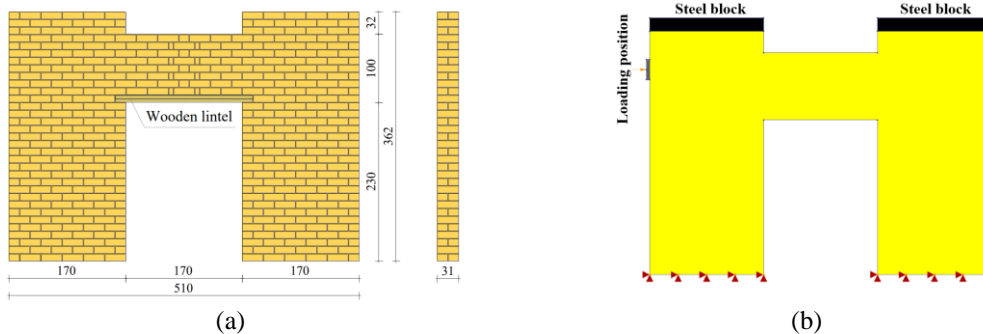


Fig. 1 – (a) Geometry and (b) FE model of the test wall (Dimensions in cm).

## 2.3 Analytical methods

The deep beam is considered a suitable structural model for solid, prismatic, and unperforated shear walls. In deep beam theory, the cross-sections are assumed to remain plane, and unlike in Bernoulli beam theory, cross-sections do not remain perpendicular to the beam axis after deformation [12]. The elastic in-plane shear stiffness of the wall can be obtained from Eq. (1) that combines the flexibility of the wall due to shear and flexure:

$$K = \frac{1}{\frac{1}{K_{flex}} + \frac{1}{K_{shear}}} \quad (1)$$

where flexural stiffnesses for a cantilevered and two fixed end walls ( $K_{flex}$ ) are calculated based on Eq. (2) and Eq. (3), respectively:

$$K_{flex} = \frac{3EI_g}{h^3} \quad (2)$$

$$K_{flex} = \frac{12EI_g}{h^3} \quad (3)$$

Moreover, the shear stiffness for a rectangular cross-section wall ( $K_{shear}$ ) is calculated from Eq. (4):

$$K_{shear} = \frac{GA_v}{1.2h} \quad (4)$$

where  $E$  is elastic modulus,  $I_g$  is the moment of inertia for the gross section,  $h$  is the height of the pier,  $G$  is the shear modulus, and  $A_v$  is the cross-section area. Two ends of a pier are not stiff enough in perforated walls to satisfy the predefined stiffness boundary conditions of Eq. (2) and Eq. (3). For the estimation of the IIPS of perforated URM walls, in this paper, two analytical methods, (a) the effective height method (EHM) and (b) the modified boundary conditions stiffness method (MBCSM), have been studied in detail.

### 2.3.1 Effective Height Method (EHM)

In EHM, the pier is divided into equally two cantilever piers, and the stiffness of each segment can be calculated based on Eq. (2). The shear stiffness of the cantilever segment is calculated based on Eq. (4), but for the flexural stiffness, Eq. (5) is utilized.

$$K_{flex} = \frac{3EI_g}{(rh)^3} \quad (5)$$

Three parameters are defined based on the geometry of the pier segment to calculate the  $r$  factor: the aspect ratio of the pier ( $\frac{W_p}{H_p}$ ), the ratio of the depth of the spandrel component to the pier ( $\frac{H_s}{W_p}$ ), and the symmetry factor of the pier end ( $\alpha$ ). The first two parameters can be calculated based on the geometry of the pier and the spandrel. The third parameter defines the asymmetry of the end region, which is described in [9]. After calculating the three mentioned parameters from the geometry of the pier and the spandrel the stiffness of the pier segments, the  $r$  factor can be derived using Eq. (6):

$$r = \left[ 1.005 + 0.19 \left( \frac{H_s}{W_p} \right)^{\frac{1}{5}} \right] \times \left[ 1 + 0.1\alpha^{\frac{1}{4}} \right] \times \left[ 0.803 + 0.281 \left( \frac{W_p}{H_p} \right)^{\frac{7}{10}} \right] \quad (6)$$

After deriving the in-plane shear stiffness of two cantilever pier segments, the IIPS of the whole pier can be calculated based on the stiffness of the top ( $K_{top}$ ) and bottom ( $K_{bot}$ ) cantilever pier segments using Eq. (7):

$$K_{pier} = \frac{1}{\frac{1}{K_{top}} + \frac{1}{K_{bot}}} \quad (7)$$

For estimating the stiffness of a perforated wall, the wall can be discretized to horizontal (spandrels) and vertical (piers) elements, as illustrated in Fig.2b. Then the stiffness of the whole wall is defined by using the series or parallel spring rules for the elements, as is shown in Fig.2c.

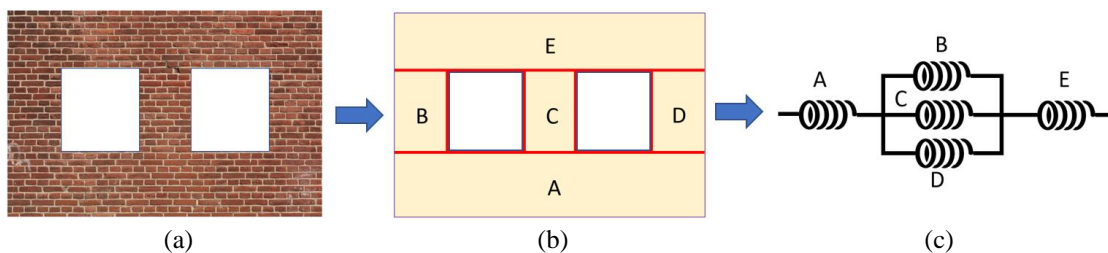


Fig. 2 – (a) A perforated URM wall, (b) dividing the wall to the spandrel and piers, and (c) composite spring model of the wall.

The IIPS of each spandrel can be roughly estimated based on Eq. (2), which  $K_{flex}$  is derived from Eq. (3), assuming a deep cantilever beam in a conservative way for all configurations of the spandrel. Then the effective stiffness of a perforated wall ( $K_{eff}$ ) is calculated as described in [9].

$K_{eff}$  is derived based on the shear stiffness of the components; however, the in-plane bending action of the wall needs to be taken into account. This effect will become larger when the wall aspect ratio increases [9]. For this purpose,  $K_{eff}$  should be modified based on Eq. (8):

$$K_{final} = \frac{1}{\frac{1}{K_{eff}} + \frac{1}{K_{bend}}} \quad (8)$$

where  $K_{bend}$  is the bending stiffness of a perforated wall and calculated based on Eq. (9):

$$K_{bend} = \frac{3EI_w}{\rho h_t^3} \quad (9)$$

In Eq. (9), the term  $I_w$  corresponds to the perforated wall's moment of inertia and  $h_t$  is the total height of the perforated wall. The term  $\rho$  is a correction factor to consider the opening effects calculated based on Eq. (10):

$$\rho = 1 + 0.0035\eta_p + 0.0004\eta_p^2 \quad (10)$$

where  $\eta_p$  is the ratio of the area of the openings to the area of the wall in percentage [9].

### 2.3.2 Modified Boundary Conditions Stiffness Method (MBCSM)

In MBCSM, the rotational deformations of the top and bottom spandrel of a pier are considered, but the shear stiffness term of Eq. (1) is not changed, and the flexural stiffness has been modified and calculated based on Eq. (11) [14]:

$$K_{flex} = \frac{6EI}{\left[ \frac{k_t k_b + 2k_t + 2k_b + 3}{k_t + k_b + 2k_t k_b} \right] \times h^3} \quad (11)$$

where  $k_b$  and  $k_t$  are equal to  $\frac{H_p}{H_{s(bottom)}}$  and  $\frac{H_p}{H_{s(top)}}$  respectively. Making the calculation procedure easier, a simplified nondimensional relationship for estimating the IIPS of a pier is introduced [14]. Firstly, three nondimensional parameters should be defined as follows:

$$q = \frac{H_p}{L} \quad (12)$$

$$s = \frac{H_{s(bottom)}}{L} \quad (13)$$

$$r = \frac{H_{s(top)}}{L} \quad (14)$$

Furthermore, the stiffness nondimensional parameter will be calculated from Eq. (15):

$$\frac{K}{Et} = \frac{1}{2pq^3 + 3q} \quad (15)$$

where the term  $p$  is calculated based on  $\frac{p_1}{p_2}$  where:

$$p_1 = 2qr + q^2 + 2qs + 3rs \quad (16)$$

and

$$p_2 = qr + 2q^2 + qs \quad (17)$$

After deriving the flexural stiffness part of the pier from Eq. (15), the pier's IIPS can be estimated based on Eq. (1) [14]. Note that the effect of asymmetry of pier ends, stiffness of spandrels and bending stiffness of the whole wall have been neglected in the MBCSM method.

#### 2.4 Developed case studies

Totally 15 walls with an equal height, including the experimental test wall (model Ex) with one, two, and three openings in different configurations, have been developed for performing the comparative study. Geometry, opening configurations, and allocated name of each case study are presented in Fig.3.

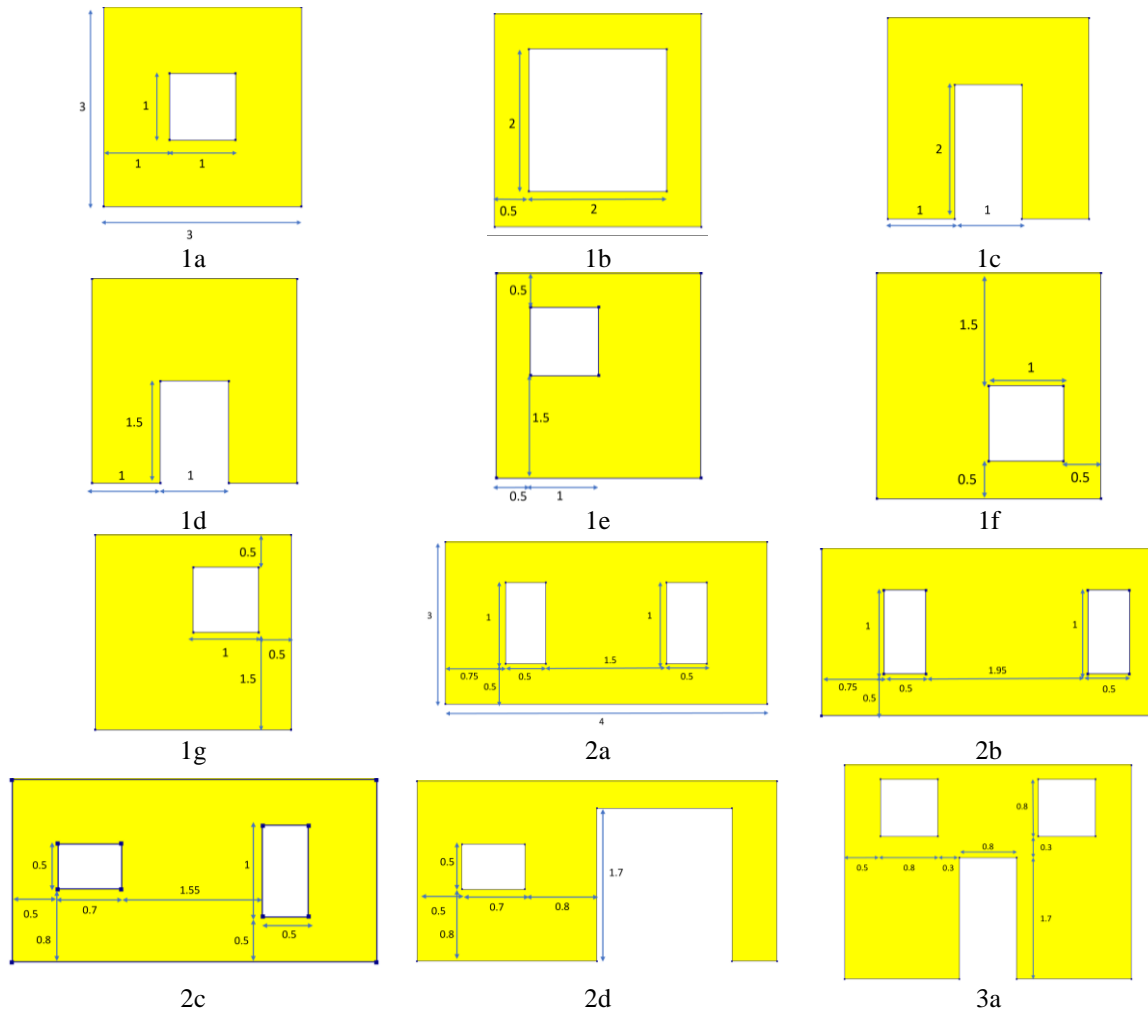




Fig. 3 – Geometry and opening configurations of the URM wall case studies (Dimensions in m).

## 2.5 Performance of the analytical methods

The IIPS of the case studies will be estimated using the two mentioned analytical methods. However, for the MBCSM, three scenarios have been considered. Firstly, the stiffness has been calculated just by summing the piers' stiffnesses. In the second scenario, the effect of spandrel stiffness has been considered (MBCSM+SE), and in the third scenario, the bending effect of the whole perforated wall is taken into account in the calculations (MBCSM+SE+BE).

### 2.5.1 Quantitative approach

The values of coefficient of determination ( $R^2$ ), root mean square error (RMSE), and mean absolute error (MAE) are calculated based on Eqs. (18), (19), and (20), respectively, to evaluate the performance of the analytical methods.

$$R^2 = \left( \frac{\sum_{j=1}^N (p_{0,j} - \bar{p}_0)(p_{t,j} - \bar{p}_t)}{\sqrt{\sum_{j=1}^N (p_{0,j} - \bar{p}_0)^2 \sum_{j=1}^N (p_{t,j} - \bar{p}_t)^2}} \right)^2 \quad (18)$$

$$\text{RMSE} = \sqrt{\frac{1}{N} \sum_{j=1}^N (p_{0,j} - p_{t,j})^2} \quad (19)$$

$$\text{MAE} = \frac{1}{N} \sum_{j=1}^N |p_{0,j} - p_{t,j}| \quad (20)$$

where  $N$  is the number of the values in both datasets,  $p_{0,j}$  and  $p_{t,j}$  are the values from two datasets and  $\bar{p}_0$  and  $\bar{p}_t$  are the corresponding mean values. It is noted that a larger value of the  $R^2$  and lower values of RMSE and MAE show a better correlation between the two datasets.

### 2.5.2 Qualitative approach

In the qualitative approach, the scatter plot of the results has been provided. The deviation of the equality line ( $Y=X$ ) from the best fitted polynomial line (i.e.,  $Y=aX+b$ ) shows the correlation of the result of each method to the obtained results from the FE analysis; and therefore, the robustness of each analytical method.

## 3. Results and discussion

### 3.1 FE model validation and mesh sensitivity analysis

The effect of mesh element size has been investigated to achieve the most efficient and accurate enough meshing size. Table 3 shows the four maximum mesh element sizes assigned to the FE model of the test wall and the corresponding number of the elements.

Table 2: Mesh sizes and the number of elements for performing the mesh sensitivity analysis.

Mesh size (m)	0.02	0.05	0.1	0.2
Number of elements	36764	5859	1466	403

A displacement with the values of 1mm has been applied on the loading position, and the IIPS is calculated as the ratio of the base shear and the prescribed displacement. Figure 12 shows the ratio of the IIPS derived from the FE model to the experimental test and the mesh sensitivity analysis results. Based on Fig.4, the maximum mesh size of 0.1 m is considered the most efficient mesh size, and the FE model is validated with adequate accuracy.

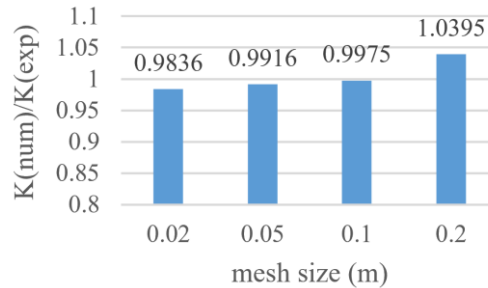
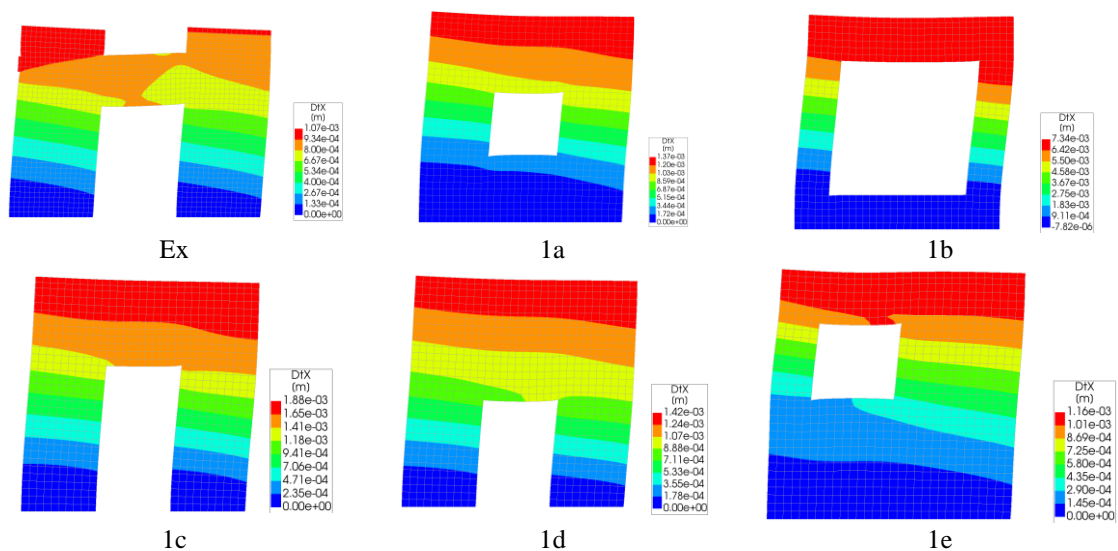


Fig. 4 – Results of the mesh sensitivity analysis.

### 3.2 FE analyses results

The material properties and the thickness of the developed case study walls are considered equal to the experimental tests. However, the elastic moduli in both X and Y directions are the same with a value of 2.07 GPa. After developing the FE models, the analysis has been done by applying a load on the top left of the wall and recording the displacement at the top right side of the wall. Based on the test procedure, a displacement-based analysis has been done for the validation of the FE model of the test wall. Nevertheless, for the analysis of the case studies, a load-based method has been utilized by applying a force and recording lateral displacement. Note that based on the previous studies on the perforated URM walls, the results from the displacement-based procedure are more conservative than the load-based procedure, see [19]. Moreover, the load-based method better reflects the loading that would be applied during a seismic event compared to the displacement-based procedure [19]. Fig.5 shows the displacement contour of the case study walls in the X direction from the FE analysis.



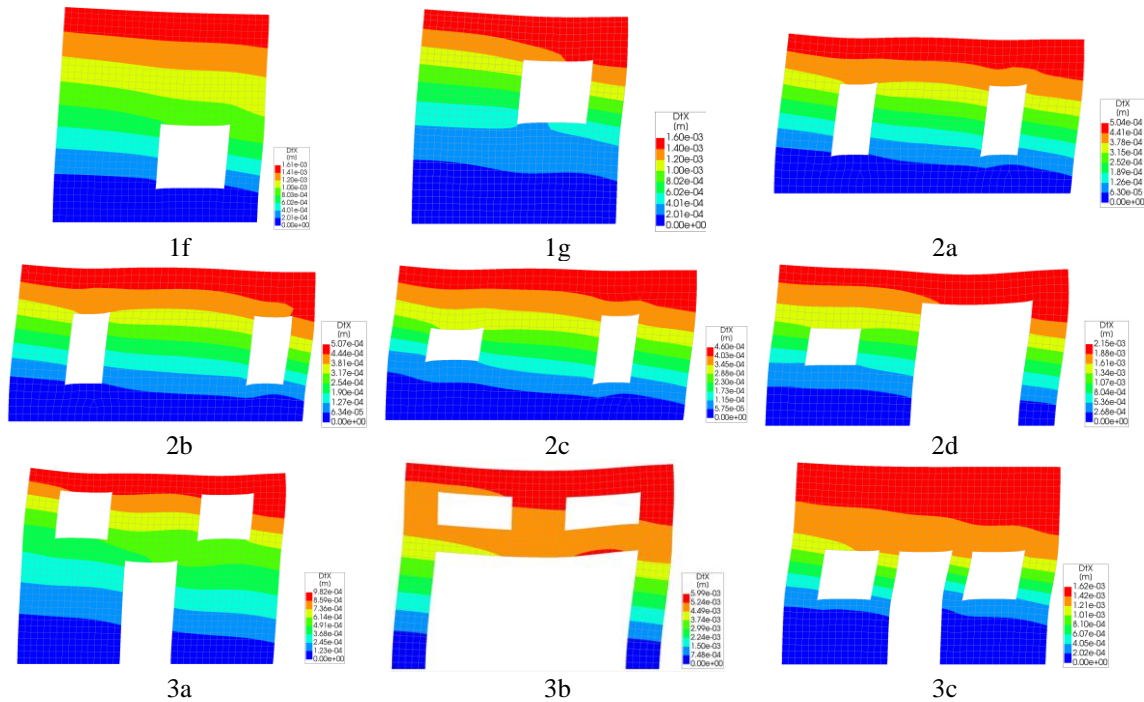


Fig. 5 – Displacement contour of the URM wall case studies in X direction obtained from FE analyses.

### 3.3 Comparative study of the perforated URM wall case studies

All the results from the FE analyses and four analytical methods have been derived, and the IIPS of the perforated URM walls are shown in Table 5. For the results from the FE analyses, the IIPS values of the case studies are calculated by dividing the applied force by the recorded displacement. The results in Table 3 show that for models 1f, 1e, and 1g, the IIPS values calculated from the analytical methods are the same, but the FE analysis results are different. Therefore, the location of opening that affects the IIPS is not effective on the results derived from the analytical methods that can be the weakness of the analytical methods. For this purpose, analytical methods for walls with symmetric configurations of openings give more accurate results.

Table 3 –IIPS of the case studies from FE analysis and the analytical methods in (kN/mm)

Model name	FE	EHM	MBCSM	MBCSM+SE	MBCSM+SE+BE
Ex	57.1817	57.0973	87.7436	72.0029	64.3741
1a	37.7489	39.4851	106.95	55.178	40.1496
1b	6.9093	6.8225	8.9125	8.5899	8.1169
1c	27.5064	26.4202	44.5625	37.276	28.755
1d	36.3148	32.7925	68.448	46.2486	34.5878
1e	44.9309	39.1383	114.4097	56.0822	40.6262
1f	32.3233	39.1383	114.4097	56.0822	40.6262
1g	32.1328	39.1383	114.4097	56.0822	40.6262
2a	104.5415	99.0443	182.9935	116.2014	105.6221
2b	103.246	101.7857	188.5906	118.4334	107.463
2c	114.7652	111.0057	318.3407	126.3638	114.1944
2d	49.1843	64.1954	157.2289	71.5514	65.5155
3a	52.7841	48.4768	53.6991	49.5441	42.5073
3b	8.9398	10.2374	10.9736	10.7159	10.0469
3c	31.6113	36.7344	48.9335	34.4814	30.8833

The values of  $R^2$ , RSME, and MAE are illustrated in Fig.6 for investigating the accuracy of each analytical method. As illustrated in Fig. 6, the value of  $R^2$  for the EHM is the largest, and the values of RSME and MAE are the lowest compared to other analytical methods. This method can be considered the most robust method compared to other analytical methods. Moreover, it is illustrated that the accuracy of the MBCSM is not enough to be employed for estimating the IIPS of URM walls. By considering the spandrel stiffness effects, the results improve, and by taking to account the bending effect stiffness, the results become more accurate. The values of  $R^2$  for EHM and modified MBCSM are 0.97 and 0.96, respectively, which confirm them as the accurate methods for estimating the IIPS of URM walls.

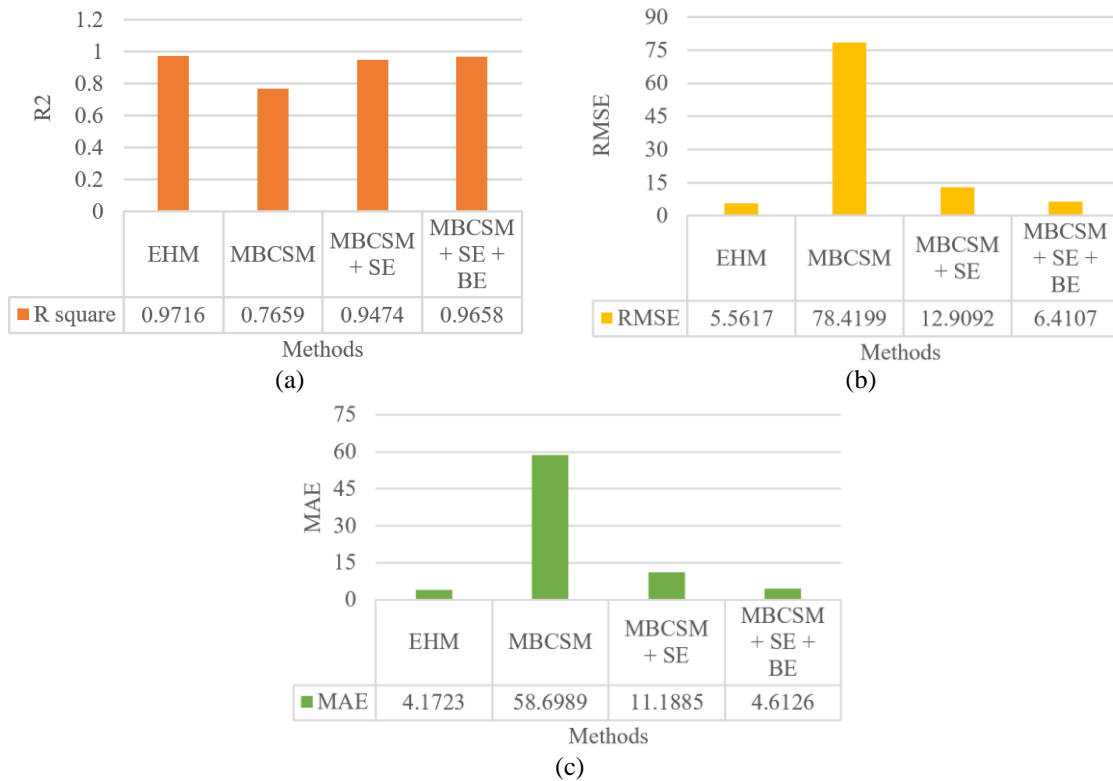
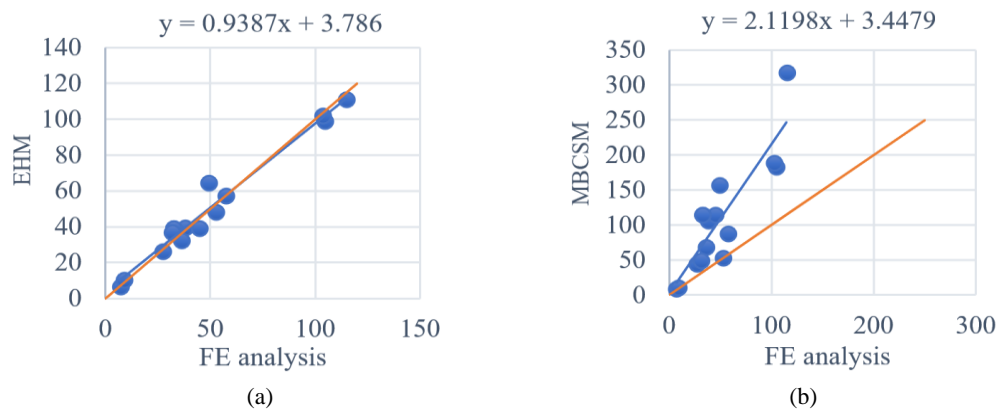


Fig. 6 – (a)  $R^2$ , (b) RMSE, and (c) MAE values for the four mentioned analytical methods.

Based on the scatter plot of EHM in Fig.7 (a), the results of EHM are accurate enough, but the best-fitted polynomial line of the MBCSM is not close enough to the equality line as illustrated in Fig.7 (b). The modifications by considering the spandrel stiffness effects and bending stiffness effects are taken into account to increase the accuracy of MBCSM that can be seen in Fig.7 (c) and (d).



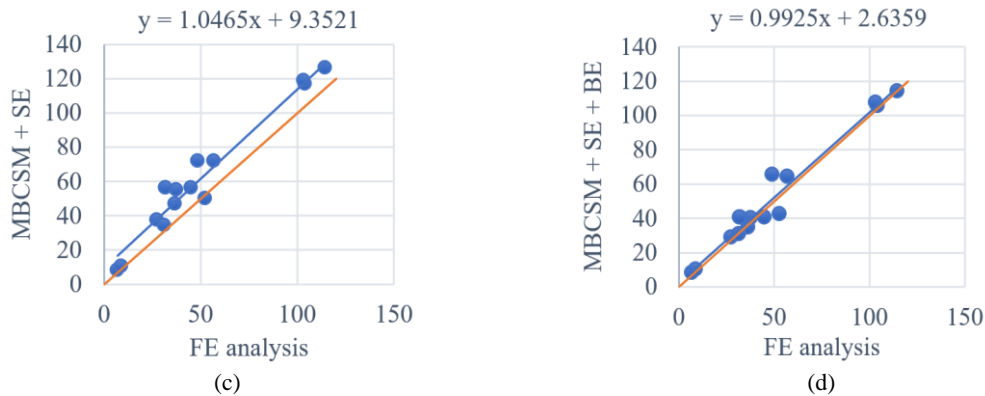


Fig. 7 – Scatter plot and the equality line for the results of FE analysis and (a) EHM, (b) MBCSM, (c) MBCSM + SE, and (d) MBCSM + SE + BE (in kN/mm).

#### 4. Conclusion

The IIPS of URM walls is considered an effective parameter on the structural vulnerability assessment of URM buildings and designing modern structural systems with URM infill walls. FE modeling is considered as a more robust method for deriving the IIPS of the URM walls with openings compared to the analytical methods. Nevertheless, expertise and high computational efforts are two main barriers that have limited the application of the FE method. Therefore, different analytical methods have been proposed for calculating the IIPS of URM walls with openings. The MBCSM and EHM are chosen as the analytical methods to investigate their performance against the FE analyses' results. For this purpose, URM wall case studies with different openings configurations have been developed, and the IIPS of the walls have been derived using the FE analyses and the mentioned analytical methods. The accuracy of each analytical method is evaluated quantitatively by calculating the RSME and MAE, and  $R^2$  parameters and qualitatively by providing the scatter plots. Performance evaluations show that results using EHM have enough accuracy but results from MBCSM show a high deviation from the FE results. Two modifications have been applied to MBCSM. Firstly, the effect of spandrel stiffness has been considered, and through the second modification, the effect of bending stiffness of the wall is added to the previous one. The comparative studies show that the modified MBCSM is accurate enough to estimate the IIPS of URM walls with openings.

#### 5. Acknowledgements

This work is a part of the HYPERION project. HYPERION has received funding from the European Union's Framework Programme for Research and Innovation (Horizon 2020) under grant agreement No 821054. The contents of this publication are the sole responsibility of Oslo Metropolitan University (Work Package 5, Task 2) and do not necessarily reflect the opinion of the European Union.

#### 6. References

- [1] Shabani, A., M. Kioumarsi, V. Plevris, and H. Stamatopoulos (2020): Structural Vulnerability Assessment of Heritage Timber Buildings: A Methodological Proposal. *Forests*. **11**(8): p. 881 <https://doi.org/10.3390/f11080881>.
- [2] D'Altri, A.M., V. Sarhosis, G. Milani, J. Rots, S. Cattari, S. Lagomarsino, E. Sacco, A. Tralli, G. Castellazzi, and S. de Miranda (2020): Modeling strategies for the computational analysis of unreinforced masonry structures: review and classification. *Archives of Computational Methods in Engineering*. <https://doi.org/10.1007/s11831-019-09351-x>.
- [3] Shabani, A., M. Kioumarsi, and M. Zucconi (2021): State of the art of simplified analytical methods for seismic vulnerability assessment of unreinforced masonry buildings. *Engineering Structures*. **239**: p. 112280 <https://doi.org/10.1016/j.engstruct.2021.112280>.

- [4] Ozturkoglu, O., T. Ucar, and Y. Yesilce (2017): Effect of masonry infill walls with openings on nonlinear response of reinforced concrete frames. *Earthquakes and Structures*. **12**(3): p. 333-347 <https://doi.org/10.12989/eas.2017.12.3.333>.
- [5] Shabani, A. and S. Erfani (2020): Seismic performance evaluation of SSMF with simple beam-column connections under the base level. *International Journal of Steel Structures*. **20**(1): p. 89-100 <https://doi.org/10.1007/s13296-019-00273-9>.
- [6] Moradi, M.J., M.M. Roshani, A. Shabani, and M. Kioumars (2020): Prediction of the load-bearing behavior of spsw with rectangular opening by RBF network. *Applied Sciences*. **10**(3): p. 1185 <https://doi.org/10.3390/app10031185>.
- [7] Bypour, M., M. Kioumars, and M. Yekrangnia (2021): Shear capacity prediction of stiffened steel plate shear walls (SSPSW) with openings using response surface method. *Engineering Structures*. **226**: p. 111340 <https://doi.org/10.1016/j.engstruct.2020.111340>.
- [8] Xu, H., C. Gentilini, Z. Yu, H. Wu, and S. Zhao (2018): A unified model for the seismic analysis of brick masonry structures. *Construction and Building Materials*. **184**: p. 733-751 <https://doi.org/10.1016/j.conbuildmat.2018.06.208>.
- [9] Craig, J.I., B.J. Goodno, Towashiraporn, and J. Park (2002): Response Modification Applications for Essential Facilities. *Georgia Institute of Technology, School of Civil and Environmental Engineering*.
- [10] Park, J., P. Towashiraporn, J.I. Craig, and B.J. Goodno (2009): Seismic fragility analysis of low-rise unreinforced masonry structures. *Engineering Structures*. **31**(1): p. 125-137 <https://doi.org/10.1016/j.engstruct.2008.07.021>.
- [11] Nicola, T., C. Leandro, C. Guido, and S. Enrico (2015): Masonry infilled frame structures: state-of-the-art review of numerical modelling. *Earthquakes and structures*. **8**(3): p. 733-759 <https://doi.org/10.12989/eas.2015.8.1.225>.
- [12] Neuenhofer, A. (2006): Lateral stiffness of shear walls with openings. *Journal of Structural Engineering*. **132**(11): p. 1846-1851 [https://doi.org/10.1061/\(ASCE\)0733-9445\(2006\)132:11\(1846\)](https://doi.org/10.1061/(ASCE)0733-9445(2006)132:11(1846)).
- [13] Qamaruddin, M., A.W. Hag, S. Al-Oraimi, and S. Hamoud (1997): Investigation on the Lateral Stiffness of Shear Walls with Openings. in *11th International Brick Block Masonry Conference, China*.
- [14] Qamaruddin, M. (1998): In-plane stiffness of shear walls with openings. *Building and Environment*. **34**(2): p. 109-127 [https://doi.org/10.1016/S0360-1323\(98\)00006-7](https://doi.org/10.1016/S0360-1323(98)00006-7).
- [15] Parisi, F., *Non-linear seismic analysis of masonry buildings*. 2010, PhD Thesis, Naples: University of Naples Federico II (URL: <http://wpage> ....
- [16] Augenti, N., F. Parisi, A. Prota, and G. Manfredi (2011): In-plane lateral response of a full-scale masonry subassembly with and without an inorganic matrix-grid strengthening system. *Journal of Composites for Construction*. **15**(4): p. 578-590 [https://doi.org/10.1061/\(ASCE\)CC.1943-5614.0000193](https://doi.org/10.1061/(ASCE)CC.1943-5614.0000193).
- [17] Croce, P., M.L. Beconcini, P. Formichi, P. Cioni, F. Landi, C. Mochi, F. De Lellis, E. Mariotti, and I. Serra (2018): Shear modulus of masonry walls: a critical review. *Procedia Structural Integrity*. **11**: p. 339-346 <https://doi.org/10.1016/j.prostr.2018.11.044>.
- [18] DIANA, *DIANA- Finite Element Analysis user manual version 10.4*. 2020: Delft, Netherlands.
- [19] Liu, Z. and A. Crewe (2020): Effects of size and position of openings on in-plane capacity of unreinforced masonry walls. *Bulletin of Earthquake Engineering*. **18**(10): p. 4783-4812 <https://doi.org/10.1007/s10518-020-00894-0>.